Magnetic Fluctuations in Pair-Density-Wave Superconductors

Morten H. Christensen,[1] Henrik Jacobsen,[1] Thomas A. Maier,[2] and Brian M. Andersen[1]

[1]*Niels Bohr Institute, University of Copenhagen, Juliane Maries Vej 30, DK-2100 Copenhagen, Denmark*
[2]*Computer Science and Mathematics Division and Center for Nanophase Materials Sciences,*
Oak Ridge National Laboratory, Oak Ridge, Tennessee 37831, USA

Pair-density-wave superconductivity constitutes a novel electronic condensate proposed to be realized in certain unconventional superconductors. Establishing its potential existence is important for our fundamental understanding of superconductivity in correlated materials. Here we compute the dynamical magnetic susceptibility in the presence of a pair-density-wave ordered state and study its fingerprints on the spin-wave spectrum including the neutron resonance. In contrast to the standard case of d-wave superconductivity, we show that the pair-density-wave phase exhibits neither a spin gap nor a magnetic resonance peak, in agreement with a recent neutron scattering experiment on underdoped $La_{1.905}Ba_{0.095}CuO_4$ [Z. Xu *et al.*, Phys. Rev. Lett. **113**, 177002 (2014)].

Superconductivity can have significant effects on the structure of the spin fluctuations. This includes, for example, the opening of a spin gap at low energies and the appearance of a magnetic neutron resonance when the gap exhibits sign changes along the Fermi surface as in cuprates and iron-based materials [1]. Similarly, the structure of the magnetic fluctuations can have important consequences for the superconducting state, even possibly its mere existence [2]. Thus, spin fluctuations and unconventional superconductivity are intimately linked, and the question of exactly how they are connected and what this tells us about the pairing mechanism [1] remains a challenging and relevant problem in the field of high-temperature superconductivity.

The pseudogap regime of the underdoped cuprates is highly susceptible to spin and charge order. Unidirectionally (striped) modulated spin and charge order was first discovered near a hole doping of $x = 1/8$ in $La_{1.6-x}Nd_{0.4}Sr_xCuO_4$ [3] and, subsequently, in other cuprates also exhibiting low-temperature tetragonal crystal structure, including $La_{2-x}Ba_xCuO_4$ [4–7]. However, stripe correlations appear to be present in many other cuprates, and the universal hourglass spin excitation spectrum observed in inelastic neutron scattering experiments has been explained within stripe models [8–10]. On the other hand, calculations based on purely itinerant models that include d-wave superconductivity but no static stripe order also find a neutron resonance with an hourglass dispersion [11]. At present, a detailed quantitative description of the spin dynamics of the cuprates and its evolution from antiferromagnetic spin waves in the parent compounds to itinerant paramagnons with a clear spin gap and a neutron resonance in the overdoped regime, remains an unsettled problem. Hence, it is important to study the intermediate doping regime where prominent stripe correlations coexist with superconducting order.

An experimental study of the transport properties of striped $La_{1.875}Ba_{0.125}CuO_4$ [12] reported 2D superconductivity coexisting with stripe order at temperatures above the 3D superconducting transition temperature. This was taken as evidence for an antiphase ordering of the superconducting order parameter between the CuO_2 layers, which suppresses the interlayer Josephson coupling required for 3D superconductivity. The existence of pair-density-wave (PDW) order, in which striped charge, magnetic, and superconducting orders are intertwined with unusual sign changes of the superconducting phase [13,14], has been proposed as a possible explanation of these findings [15,16]. In the PDW state, the superconducting order parameter has a finite Cooper pair momentum with periodicity equal to that of the magnetic stripe order as illustrated in Fig. 1(a) [17]. This is to be contrasted with a more ordinary modulated d-wave superconductor (dSC), in which the superconducting order parameter is in phase across the stripe domains and modulated in amplitude with the same periodicity as the charge stripes, i.e., half the wavelength of the PDW state as shown in Fig. 1(b).

The possibility of a PDW state was investigated within microscopic models, and numerical studies of the t-J model generally find that this state is energetically competitive with other more ordinary modulated superconducting states [18–21]. Similar conclusions were reached within an extended version of BCS theory above a critical pairing strength [22], while subsequent Hartree-Fock studies focused on the single-particle electronic properties of phases of combined PDW order and antiferromagnetic stripes [23,24]. More recently, finite momentum superconducting PDW order has resurfaced in theoretical studies of the charge density wave (CDW) order detected in underdoped cuprates [25–27]. The existence of an entangled CDW + PDW phase was found and analyzed

both in the context of an emergent SU(2) symmetry of the fermionic hot-spot model [27,28] and in the spin-fermion model close to the onset of antiferromagnetism [29,30].

Experimentally, a recent neutron scattering study of the low-energy spin response in stripe ordered $La_{1.905}Ba_{0.095}CuO_4$ [31] found a number of remarkable results that were taken as evidence for a PDW state: (1) gapless spin excitations coexisting with superconductivity and (2) the absence of a neutron resonance in the superconducting state. These results are highly unusual since both a spin gap and a neutron resonance are expected in unconventional superconductors like the cuprates [1].

Motivated by the experimental findings of Ref. [31], we perform a theoretical study of the fingerprints of a putative PDW state on the inelastic neutron scattering spectrum. We focus on the consequences of the PDW state rather than its microscopic origin. We find that the PDW state in the *absence* of magnetic and charge order exhibits neither a spin gap nor a neutron resonance, contrary to the standard dSC phase. For the state where PDW superconductivity coexists with striped magnetic order, we find qualitatively similar results. In particular, the neutron scattering spectrum in this coexistence phase is almost identical to that of the normal state. In the standard dSC phase, on the other hand, we show that the neutron resonance is robust to coexisting stripe order. These findings support a scenario where the absence of a spin gap and a magnetic resonance in underdoped $La_{1.905}Ba_{0.095}CuO_4$ [31] is explained by the existence of a PDW condensate.

The stripe phase coexisting with superconductivity is studied within a phenomenological mean-field one-band Hubbard model

$$\mathcal{H}^{MF} = -\sum_{ij\sigma}(t_{ij} + \mu\delta_{ij})c_{i\sigma}^\dagger c_{j\sigma} + U\sum_{i\sigma}\langle n_{i\bar\sigma}\rangle n_{i\sigma}$$
$$- \sum_{\langle ij\rangle}[\Delta_{ji}c_{i\uparrow}^\dagger c_{j\downarrow}^\dagger + \text{H.c.}], \qquad (1)$$

with $U > 0$. For the hopping integrals t_{ij}, we include nearest-neighbor $t = 1$ (setting the unit of energy) and next-nearest-neighbor $t' = -0.3$. The details of the band structure are not important for the results discussed below. The associated Fermi surface of the tight-binding model is depicted in Fig. 1(c). The Hamiltonian (1) and its generalizations have been used previously to study the stripe phase of the cuprates [32–35], including the electronic properties of the PDW phase [23,24], but an analysis of the spin response in the PDW phase has not previously been addressed theoretically.

Here we use an 8×2 supercell to study the effects of stripe and PDW order on the magnetic excitation spectrum. The periodicity of the magnetic (charge) stripe order is, therefore, restricted to 8 (4) lattice sites along $\hat{x}$ and 2 (1) sites along $\hat{y}$. This restriction limits the possible solutions, and a self-consistent iterative procedure, in
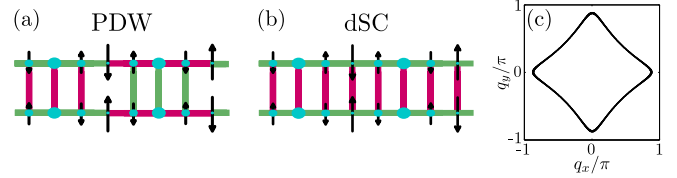

FIG. 1. (a),(b) Illustration of the unit cells with charge and spin order, and either PDW (a) or dSC (b) superconducting order. The arrows denote the magnetization, the diameter of the circles the hole density, and the colors on the bonds indicate the sign of the superconducting order parameter; green is positive and magenta is negative. (c) Normal state Fermi surface with a doping of 12.5%.

general, only obtains a saddle point in the free energy landscape. The actual minimum is often located at a different periodicity which is inaccessible due to the restriction to (8×2)-periodic unit cells. In such cases, the Goldstone modes either remain gapped, or the spin-wave branches cross zero energy before reaching the ordering vector [36]. To study the spin response in the presence of (8×2)-periodic stripes, we, therefore, adopt an alternative approach: we impose a density modulation $\langle n_{i\sigma}\rangle$ corresponding to site-ordered magnetic and charge stripes and a superconducting order parameter $|\Delta_{ij}| = 0.05$ corresponding to either dSC or PDW order, as shown in Figs. 1(a) and 1(b). For each chosen configuration, we subsequently adjust the bare interaction U such that Goldstone's theorem is satisfied, i.e., such that the denominator of the real part of the RPA susceptibility exhibits a zero eigenvalue at $q_x = \pi \pm (\pi/4)$ (see the Supplemental Material [37] for further details). This procedure guarantees a stable energy minimum in the energy landscape of (8×2)-periodic stripes and has the benefit of allowing us to study PDW-, dSC-, and nonsuperconducting solutions within the same region of parameter space and the same assumed density modulations. Furthermore, this allows us to single out the effects of just the PDW order on the spin susceptibility.

We apply a supercell formalism, where the total $N \times N$ (here $N = 96$) system consists of supercells of size 8×2. The dynamic spin susceptibility $\chi^{+-}(\mathbf{q},\omega) = \chi^{+-}(\mathbf{q}, i\omega_n \to \omega + i\delta)$ that determines the neutron scattering intensity may be obtained from

$$\chi^{+-}(\mathbf{q}, i\omega_n) = \sum_{\mathbf{r}_i,\mathbf{r}_j} e^{-i\mathbf{q}(\mathbf{r}_i-\mathbf{r}_j)}\chi^{+-}(\mathbf{r}_i, \mathbf{r}_j, i\omega_n), \qquad (2)$$

which contains terms originating from both the intra- and intersupercell structure. Here, $\mathbf{r}_i = \mathbf{R}_i + i$ where $\mathbf{R}_i$ yields the supercell containing site $\mathbf{r}_i$ and i gives the site of $\mathbf{r}_i$ in that supercell. The site-dependent susceptibility is obtained from

$$\chi^{+-}(\mathbf{r}_i, \mathbf{r}_j, i\omega_n) = \int_0^\beta d\tau e^{i\omega_n\tau}\langle S^+(\mathbf{r}_i, \tau)S^-(\mathbf{r}_j, 0)\rangle, \qquad (3)$$

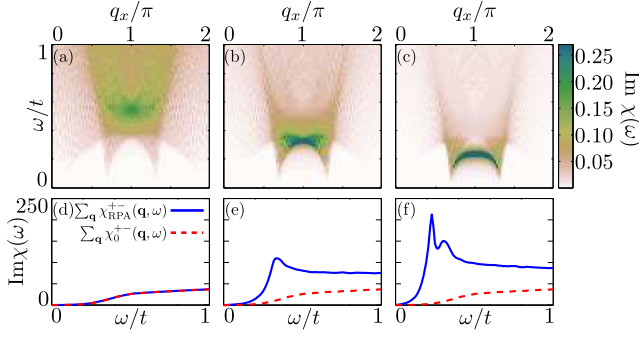FIG. 2. (a)–(c) Imaginary part of the spin susceptibility Im$\chi^{+-}(\mathbf{q}, \omega)$ with only dSC order. Here we have set $q_y = \pi$ and plot Im$\chi^{+-}(q_x, \pi, \omega)$ versus q_x/π and ω/t with (a) $U = 0$, (b) $U/t = 1.8$, and (c) $U/t = 2.2$. For clarity, the intensity of the first two cases has been rescaled. (d)–(f) show the imaginary part of the $\mathbf{q}$-integrated bare (red dashed) and RPA (blue solid lines) susceptibilities.

FIG. 3. (a)–(c) Imaginary part of the spin susceptibility Im$\chi^{+-}(\mathbf{q}, \omega)$ versus q_x/π and ω/t for a system with only PDW order for the same values of U as in Fig. 2. (d)–(f) Imaginary part of the $\mathbf{q}$-integrated susceptibilities corresponding to (a)–(c). The black dashed lines show the integrated RPA susceptibility in the normal state.

where $S^+(\mathbf{r}_i, \tau) = c^{\dagger}_{\mathbf{r}_i\uparrow}(\tau)c_{\mathbf{r}_i\downarrow}(\tau)$ is the spin raising operator at position $\mathbf{r}_i$ at (imaginary) time τ and $S^-(\mathbf{r}_i, \tau)$ the corresponding spin lowering operator. The bare susceptibility takes the standard form consisting of contributions from both normal and anomalous Green functions as detailed in the Supplemental Material [37]. At the RPA level, the site-dependent susceptibility is given by

$$\chi^{+-}(\mathbf{r}_i, \mathbf{r}_j, \omega) = \chi_0^{+-}(\mathbf{r}_i, \mathbf{r}_j, \omega)$$
$$+ U \sum_{\mathbf{r}_l} \chi_0^{+-}(\mathbf{r}_i, \mathbf{r}_l, \omega)\chi^{+-}(\mathbf{r}_l, \mathbf{r}_j, \omega), \quad (4)$$

where $\chi_0^{+-}(\mathbf{r}_i, \mathbf{r}_j, \omega)$ is the bare susceptibility calculated with respect to the mean-field Hamiltonian in Eq. (1).

In order to disentangle the effects of superconductivity on the spin response from those of the striped magnetic order, we start by considering systems with either only dSC or only PDW order, i.e., without coexisting charge and magnetic order. In Fig. 2 we show the imaginary part of the RPA susceptibility for the dSC phase at $q_y = \pi$. As evident from the results for the bare susceptibility χ_0 (red dashed curve) in Figs. 2(c) and 2(d), one clearly sees the opening of a spin gap below 2Δ (at $U = 0$). At finite U, a resonance peak, which shifts to lower energies as U increases, appears at energies slightly below the bare spin gap as seen more clearly from Figs. 2(e) and 2(f), as expected for a superconducting gap that changes sign under translation of $\mathbf{Q} = (\pi, \pi)$ [1,11].

The corresponding results for the case with only PDW order are plotted in Fig. 3 and seen to be in stark contrast to the phase with only dSC order (Fig. 2). In the PDW phase, although the system is superconducting, a spin gap is clearly absent. Without a spin gap, quasiparticle damping is not suppressed, which further implies that a magnetic resonance should be absent, consistent with the RPA results
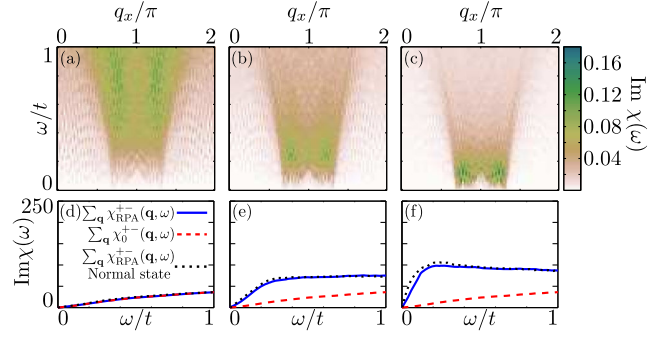
displayed in Fig. 3. As seen, the spectral weight is rather structureless and distributed over a wider range in both frequency and momentum. A comparison of the PDW phase with the normal (nonordered) case shown in Figs. 3(d)–(f) by the dotted black lines reveals that the spin response of the normal state and the PDW state are, in fact, remarkably similar.

One may understand the absence of a spin gap in the PDW state from the zero frequency single-particle spectral weight $\mathcal{A}(\mathbf{k}, \omega = 0)$ and the associated density of states (DOS) displayed in Figs. 4(a) and 4(d). The dSC phase (not shown) exhibits the usual gap structure, with gap nodes along the $|k_x| = |k_y|$ lines in $\mathcal{A}(\mathbf{k})$. In contrast, the PDW phase exhibits states on large parts of the Fermi surface [Fig. 4(a)], and the DOS clearly does not exhibit a suppression of states near the Fermi level [24]. The
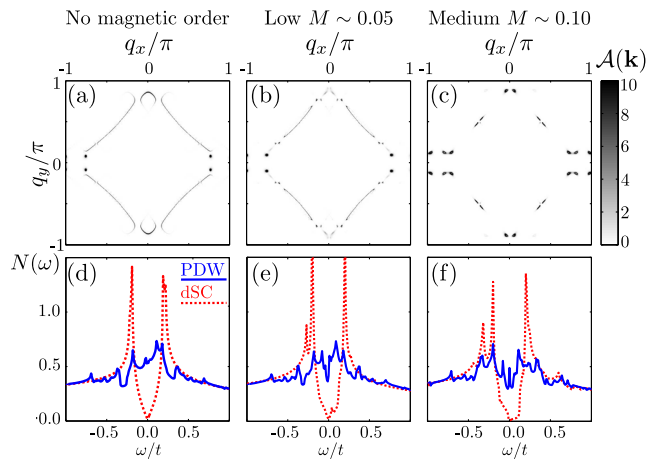

FIG. 4. (a)–(c) The spectral function $\mathcal{A}(\mathbf{k}, \omega = 0)$ for a system with PDW order and increasing magnitude of the site-averaged magnetic moment. (d)–(f) Comparison of the DOS for the PDW and dSC phases for the same parameters corresponding to panels (a)–(c).
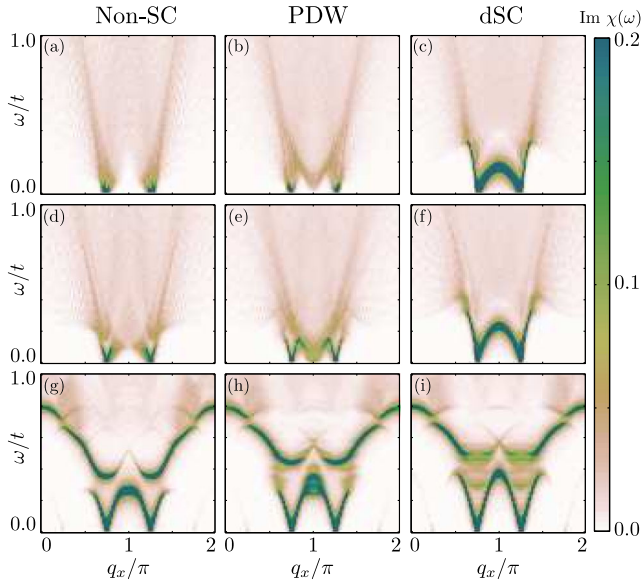
FIG. 5.   Imaginary part of the spin susceptibility $\mathrm{Im}\chi^{+-}(\mathbf{q}, \omega)$ in the presence of stripe charge and magnetic order without superconductivity (left column) and with superconductivity (middle and rightmost columns) for increasing magnetic order; (a)–(c) show the case where the site-averaged magnetic moment $M \sim 0.05$, (d)–(f) correspond to $M \sim 0.1$, and (g)–(i) have $M \sim 0.4$.
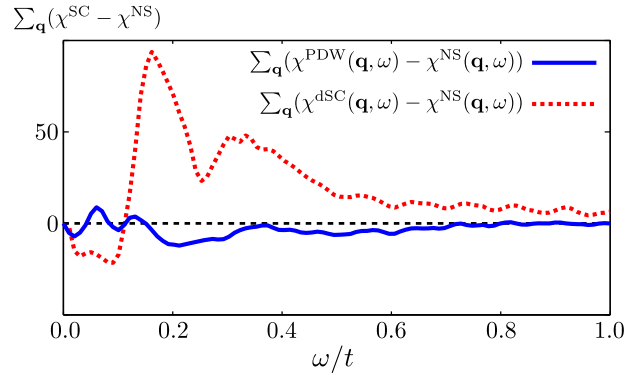

FIG. 6.   Comparison of the integrated neutron resonance for the PDW and dSC cases. The blue curve shows the difference between the PDW and the nonsuperconducting case, while the red curve shows the difference between the dSC case and the nonsuperconducting case. The dSC shows clear signs of a resonance, which is absent for the PDW case.

low-energy states in the PDW state are caused by the mismatch of the real-space pairing bonds seen in Fig. 1(a), which are known to produce low-energy Andreev-like zero-energy states [38].

We now turn to the full coexistence phase with (8 × 2)-periodic magnetic and charge stripes as well as PDW or dSC orders present. Combining superconductivity with magnetic and charge order leads to a reconstruction of the Fermi surface evidenced in Figs. 4(b) and 4(c). The effect of a finite (weak) magnetization on the DOS is relatively minor, as seen in Figs. 4(e) and 4(f). The system with a PDW does not exhibit a full gap, even at $\omega = 0$, while the gap present in the dSC case is only altered quantitatively by the addition of magnetism. Similar conclusions hold for the spectral function: the PDW state still exhibits states on large parts of the Fermi surface, while only states along the nodal lines are present in the dSC phase.

Proceeding to study the spin-wave spectrum of the coexistence phase, we first note that the presence of Goldstone modes necessarily excludes the opening of a spin gap. This is clearly seen in Fig. 5, where we show the imaginary part of the susceptibility $\chi^{+-}(\mathbf{q}, \omega)$ versus q_x with $q_y = \pi$ for an increasing magnitude of the site-averaged magnetic moment. The Goldstone modes are seen by the high intensity peaks at $\omega = 0$ for $q_x = \pi \pm \pi/4$ for all the cases shown. Figures 5(a)–(c) correspond to a site-averaged magnetic moment of $M \sim 0.05$, Figs. 5(d)–(f) have $M \sim 0.1$ [39], and Figs. 5(g)–(i) have $M \sim 0.4$ (see the

Supplemental Material [37] for the exact order parameters used). In the dSC phase, there is still a resonance indicated by the region of high intensity at $q_x = \pi$ visible as the region of high intensity bridging the two spin-wave branches as seen most clearly in Figs. 5(c) and 5(f). This is in stark contrast to the PDW case [Figs. 5(b) and 5(e)] where this coherent excitation is completely washed out, similar to the case shown in Fig. 3 without charge and spin order. For larger magnetic moments, the magnetic excitations approach the standard spin-wave branches of the stripe phase [40–42], but a significantly broadened dispersion at the resonance point ($q_x = \pi$) is seen to remain present in the PDW phase compared to the dSC phase, as seen by comparison of Figs. 5(h) and 5(i).

To illustrate this more clearly, we show in Fig. 6 the difference in the $\mathbf{q}$-integrated spin susceptibility between the superconducting and normal state for both the PDW (solid blue) and dSC orders (dotted red). These results are for the case where the site-averaged magnetic moment $M \sim 0.1$ [Figs. 5(d)–(f)]. As seen, the dSC phase exhibits a clear resonance around $\omega/t \sim 0.18$, while the PDW phase is structureless. In fact, the PDW case has an almost identical spin response to the normal state, a result that is in good agreement with the experimental data measured on LBCO at $x = 0.095$ by Xu et al. [31].

To summarize, we have studied the distinct signatures of a PDW state with intertwined striped spin, charge, and antiphase superconducting bond order on the dynamic spin susceptibility. We have found that in the PDW state both a spin gap and a neutron resonance are absent, in contrast to the coexistence phase with standard in-phase d-wave superconductivity where the neutron resonance is preserved. This absence of the usual fingerprint of a sign-changing superconducting gap in the PDW state can be traced back to its gapless single-particle excitation spectrum. These results are in agreement with recent neutron

scattering results on $x = 0.095$ LBCO [31], where neither a spin gap nor a resonance were observed below the superconducting critical temperature.

[1] D. J. Scalapino, Rev. Mod. Phys. **84**, 1383 (2012).
[2] N. F. Berk and J. R. Schrieffer, Phys. Rev. Lett. **17**, 433 (1966).
[3] J. M. Tranquada, B. J. Sternlieb, J. D. Axe, Y. Nakamura, and S. Uchida, Nature (London) **375**, 561 (1995).
[4] H.-H. Klauss, W. Wagener, M. Hillberg, W. Kopmann, H. Walf, F. J. Litterst, M. Hücker, and B. Büchner, Phys. Rev. Lett. **85**, 4590 (2000).
[5] M. Fujita, H. Goka, K. Yamada, J. M. Tranquada, and L. P. Regnault, Phys. Rev. B **70**, 104517 (2004).
[6] J. Fink, E. Schierle, E. Weschke, J. Geck, D. Hawthorn, V. Soltwisch, H. Wadati, H.-H. Wu, H. A. Dürr, N. Wizent, B. Büchner, and G. A. Sawatzky, Phys. Rev. B **79**, 100502(R) (2009).
[7] M. Hücker, M. v. Zimmermann, G. D. Gu, Z. J. Zu, J. S. Wen, G. Xu, H. J. Kang, A. Zheludev, and J. M. Tranquada, Phys. Rev. B **83**, 104506 (2011).
[8] S. A. Kivelson, E. Fradkin, V. Oganesyan, J. M. Tranquada, A. Kapitulnik, and C. Howald, Rev. Mod. Phys. **75**, 1201 (2003).
[9] J. M. Tranquada, in *Handbook of High-Temperature Superconductivity Theory and Experiment*, edited by J. R. Schrieffer (Springer, New York, 2007).
[10] M. Vojta, Adv. Phys. **58**, 699 (2009).
[11] M. Eschrig, Adv. Phys. **55**, 47 (2006).
[12] Q. Li, M. Hücker, G. D. Gu, A. M. Tsvelik, and J. M. Tranquada, Phys. Rev. Lett. **99**, 067001 (2007).
[13] D. F. Agterberg and H. Tsunetsugu, Nat. Phys. **4**, 639 (2008).
[14] S. Baruch and D. Orgad, Phys. Rev. B **77**, 174502 (2008).
[15] E. Berg, E. Fradkin, E.-A. Kim, S. A. Kivelson, V. Oganesyan, J. M. Tranquada, and S. C. Zhang, Phys. Rev. Lett. **99**, 127003 (2007).
[16] E. Berg, E. Fradkin, and S. A. Kivelson, Phys. Rev. B **79**, 064515 (2009).
[17] E. Fradkin, S. A. Kivelson, and J. M. Tranquada, Rev. Mod. Phys. **87**, 457 (2015).
[18] A. Himeda, T. Kato, and M. Ogata, Phys. Rev. Lett. **88**, 117001 (2002).
[19] M. Raczkowski, M. Capello, D. Poilblanc, R. Frésard, and A. M. Oleś, Phys. Rev. B **76**, 140505 (2007).
[20] K.-Y. Yang, W. Q. Chen, T. M. Rice, M. Sigrist, and F.-C. Zhang, New J. Phys. **11**, 055053 (2009).
[21] P. Corboz, T. M. Rice, and M. Troyer, Phys. Rev. Lett. **113**, 046402 (2014).
[22] F. Loder, A. P. Kampf, and T. Kopp, Phys. Rev. B **81**, 020511(R) (2010).
[23] F. Loder, S. Graser, A. P. Kampf, and T. Kopp, Phys. Rev. Lett. **107**, 187001 (2011).
[24] F. Loder, S. Graser, M. Schmid, A. P. Kampf, and T. Kopp, New J. Phys. **13**, 113037 (2011).
[25] P. A. Lee, Phys. Rev. X **4**, 031017 (2014).
[26] Y. Wang and A. Chubukov, Phys. Rev. B **90**, 035149 (2014).
[27] C. Pépin, V. S. de Carvalho, T. Kloss, and X. Montiel, Phys. Rev. B **90**, 195207 (2014).
[28] H. Freire, V. S. de Carvalho, and C. Pépin, Phys. Rev. B **92**, 045132 (2015).
[29] Y. Wang, D. F. Agterberg, and A. Chubukov, Phys. Rev. Lett. **114**, 197001 (2015).
[30] Y. Wang, D. F. Agterberg, and A. V. Chubukov, Phys. Rev. B **91**, 115103 (2015).
[31] Z. Xu, C. Stock, S. Chi, A. I. Kolesnikov, G. Xu, G. Gu, and J. M. Tranquada, Phys. Rev. Lett. **113**, 177002 (2014).
[32] J.-X. Zhu, I. Martin, and A. R. Bishop, Phys. Rev. Lett. **89**, 067003 (2002).
[33] Y. Chen and C. S. Ting, Phys. Rev. Lett. **92**, 077203 (2004).
[34] B. M. Andersen and P. Hedegård, Phys. Rev. Lett. **95**, 037002 (2005).
[35] B. M. Andersen, S. Graser, and P. J. Hirschfeld, Phys. Rev. Lett. **105**, 147002 (2010).
[36] B. Dalla Piazza, M. Mourigal, N. B. Christensen, G. J. Nielsen, P. Tregenna-Piggott, T. G. Perring, M. Enderle, D. F. McMorrow, D. A. Ivanov, and H. M. Rønnow, Nat. Phys. **11**, 62 (2015).
[37] See the Supplemental Material at http://link.aps.org/supplemental/10.1103/PhysRevLett.116.167001 for details of the calculations and specifics of the approach.
[38] B. M. Andersen, A. Melikyan, T. S. Nunner, and P. J. Hirschfeld, Phys. Rev. Lett. **96**, 097004 (2006).
[39] In the two cases in Figs. 5(a)–(c) and Figs. 5(d)–(f), a slightly different value of $t' = -0.22$ was used to facilitate the satisfaction of Goldstone's theorem.
[40] F. Krüger and S. Scheidl, Phys. Rev. B **67**, 134512 (2003).
[41] G. Seibold and J. Lorenzana, Phys. Rev. B **73**, 144515 (2006).
[42] D. X. Yao, E. W. Carlson, and D. K. Campbell, Phys. Rev. B **73**, 224525 (2006).